Vortex structure and dynamics in YNi_2B_2C single crystal by ^{11}B NMR

K. H. Lee, B. J. Mean, G. S. Go, S. W. Seo, K. S. Han, D. H. Kim,
and Moohee Lee*
Department of Physics and Center for Advanced Materials and Devices, Konkuk University, Seoul 143-701, Korea

B. K. Cho
Department of Material Science and Technology, Kwangju Institute of Science and Technology, Kwangju 500-712, Korea

S. I. Lee
National Creative Initiative Center for Superconductivity, POSTECH, Pohang, Kyung-Buk 790-784, Korea
(Received 27 March 2000)

^{11}B NMR measurements have been performed on a single crystal of YNi_2B_2C superconductor to investigate the vortex structure and dynamics. Below T_c, the ^{11}B NMR spectrum, shift, linewidth, and transverse relaxation rate $1/T_2$ exhibit distinct features from which three vortex phases are identified, namely, vortex liquid, glass, and lattice. Also, thermal hysteresis of the saddle-point field, motional narrowing of linewidth, and double-peak structure of $1/T_2$ altogether indicate significant thermal motion of vortices in this low T_c and nearly isotropic three-dimensional superconductor.

Numerous important research results have been reported on exotic vortex structures and dynamics in RNi_2B_2C superconductors. These include the controversial vortex melting[1] and a transition from triangular to square vortex lattices.[2] Vortex dynamics for RNi_2B_2C were probed by transport measurements,[1] scanning tunnel microscopy,[3] and small-angle neutron scattering experiments.[4–6]

Recently, NMR experiments have played an essential role in understanding vortex dynamics in cuprate superconductors[7–14] since NMR is sensitive to the local field distributions and fluctuations. Those measurements include ^{63}Cu (Ref. 8), ^{17}O (Ref. 9–11), ^{89}Y (Refs. 11–13), and ^{203}Tl (Ref. 14) NMR for aligned powder samples. In contrast to the cuprates, RNi_2B_2C (R=rare earth elements) systems have low T_c and H_{c2} and are nearly isotropic three-dimensional (3D) superconductors. Therefore, the vortex structure and dynamics in RNi_2B_2C are particularly interesting. Consequently, it is important to investigate it further, both static and dynamical porperties, using NMR.

In this paper, we report NMR measurements on vortex dynamics in RNi_2B_2C. Our ^{11}B NMR results show characteristic features depending on temperature, which enable us to identify three vortex phases: *vortex liquid, glass, and lattice*. We have observed thermal hysteresis of the Knight shift as a signature of a vortex glass. Furthermore, pinning effects are exhibited in NMR data in the form of a reduction of $1/T_2$ near T_c. From detailed analysis of NMR data, microscopic and quantitative information regarding time and length scales of vortex distortion and fluctuation are provided.

YNi_2B_2C single crystals were grown by the Ni_2B high-temperature flux growth method.[15] As-grown crystals were of platelike shape with the c axis perpendicular to the plate plane. The crystal used for this measurement was $\approx 11\times 8\times 2$ mm^3 in size. Pulsed ^{11}B NMR measurements were performed down to 3.8 K for magnetic fields 1–5 T parallel to the c axis.

In the mixed state of type-II superconductors, vortices at low temperature form a lattice generating a spatial field modulation. An average vortex spacing for the square lattice is $d=\sqrt{\Phi_0/H_{ext}}$, where Φ_0 is the flux quantum and H_{ext} is the external field. d is 333 Å at 1.8 T. The NMR spectrum is the local-field distribution at the probing nuclear sites.

^{11}B NMR spectra at 3 T are plotted in Fig. 1. The spectrum at $T=3.8$ K in Fig. 1(a) exhibits a typical asymmetric shape, confirming the *lattice formation of vortices*. Namely, vortices are equilibrated at the regular lattice points. The inset of Fig. 1(a) shows the calculated NMR spectrum in the vortex lattice state with minimum field H_m, saddle-point field H_s, and maximum field H_M at the vortex core. Defining $\beta\equiv(H_s-H_m)/(H_M-H_m)$, two types of vortex state, i.e., triangular and square lattices, can be distinguished; $\beta=0.07$ for the triangular lattice and $\beta=0.29$ for the square lattice.[16] For YNi_2B_2C, $\beta=0.24\pm 0.05$ is found, which suggests that the vortex lattice at $H=3$ T parallel to the c axis is a *square* type, consistent with other published reports.[4–6]

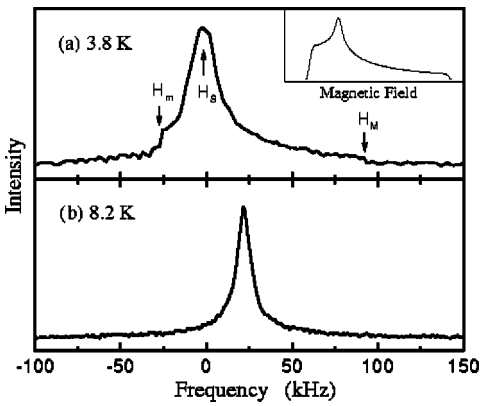

FIG. 1. ^{11}B NMR spectra of YNi_2B_2C single crystal at 3 T ($T_c=9.4$ K): (a) $T=3.8$ K (b) $T=8.2$ K. Inset: calculated-field distribution for the square vortex lattice.

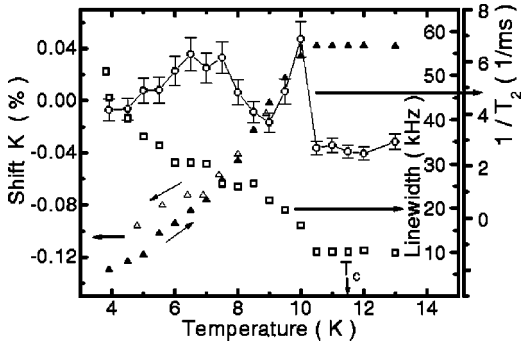

FIG. 2. ^{11}B NMR data of YNi_2B_2C single crystal at $H=1.8$ T ($T_c=11.5$ K) parallel to the c axis. Filled triangles, Knight shift with slowly warming up from low-temperature equilibrium; open triangles, Knight shift with fast cooling down after first measurements; squares, linewidth; and circles, $1/T_2$. The line on $1/T_2$ is a guide to the eye.

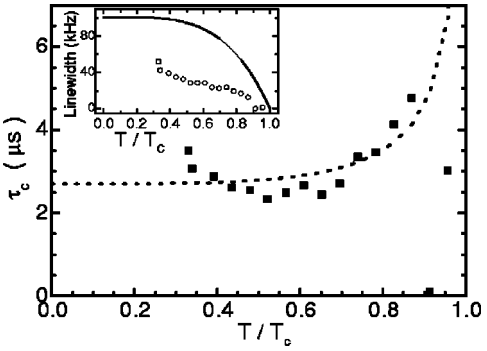

FIG. 3. Characteristic time scale of vortex fluctuation extracted from the motional narrowing of linewidth as in the inset. Dotted line is a fit to a model (see text). Inset: the measured linewidth solely due to the vortices, Δf_v (circles), and the expected linewidth for the rigid vortex lattice (line).

The square-type lattice is also observed at $H=1.0$ and 1.8 T down to $T=3.8$ K. Therefore, these results are consistent with the theoretical calculation,[2] according to which the structural change from triangular to square lattices appears at a much lower magnetic field.

Above 4 K and up to T_c the line shape gradually changes to a symmetric narrow resonance, as shown in Fig. 1(b), which indicates that the flux lines fluctuate thermally and are distorted from the equilibrium lattice points forming a *vortex glass* (in the generic meaning of glass). The formation of a vortex glass is also evident from *thermal hysteresis* of ^{11}B NMR shift, as shown in Fig. 2, which will be discussed later.

Figure 2 shows ^{11}B NMR shift, linewidth, and $1/T_2$ as a function of temperature. Although T_c at 1.8 T is measured to be 11.5 K from temperature-dependent resistance,[1] all three NMR data start to reveal a sharp change below $T=10.5$ K. All NMR data for $10.5\text{K}\leqslant T\leqslant T_c$ are indistinguishable from the normal state values. The same behavior has been observed and interpreted as a signature of the vortex liquid state in high-T_c cuprate superconductors,[8–11] where the temperature range for the vortex liquid state is quite large due to the two-dimensional nature of the vortex. It is believed that, in the vortex liquid phase, vortex motion is so rapid that the spatial variation of the field from vortices is averaged out in NMR.[8,11]

The Knight shift in the normal state is almost temperature independent and consistent with the published report.[17] The shift changes abruptly below $T=10.5$ K in the superconducting state. The total shift in the superconducting state consists of spin, orbital and diamagnetic shifts; $K_{\text{tot}}=K_{\text{spin}}+K_{\text{orb}}+K_{\text{dia}}$. Since the three contributions have different field and temperature dependence we can, in principle, separate out each contribution to the total shift, respectively. From the field dependence of the total shift we found that $K_{\text{spin}}+K_{\text{orb}}$ is less than 0.03% down to 3.8 K (Ref. 18) and consequently, the observed shift in the superconducting state is mainly due to the diamagnetic shift reflecting the saddle-point field. As can be seen in Fig. 2, there is thermal hysteresis of the ^{11}B NMR shift between gradual warming (filled triangle) and rapid cooling (open triangle). The thermal hysteresis of the shift proves that the flux lines fluctuating with a large amplitude at high temperature are frozen at the pinning sites during the rapid cooling process and are not recovered back to the original positions at low temperature, indicating that vortices are in a *glass* state.

$1/T_2$ in Fig. 2 is independent of temperature in the normal state. In the superconducting state, however, $1/T_2$ shows strong temperature dependence with a double-peak structure. $1/T_2$ is measured from the decay time constant of spin-echo signals, which are formed by two pulses separated by the echo formation time τ_e. The echo formation is based on the condition that local fields remain unchanged during the dephasing period of τ_e after the first pulse and during the refocusing period of τ_e after the second pulse. If, however, the local field fluctuates due to flux-line motion, then the echo is not completely refocused resulting in a faster decay of the echo height and leading to a shorter T_2. Thus $1/T_2$ is proportional to the fluctuating local field $\langle h_z^2\rangle$, and sensitively probes the slow motion of vortices in the time scale of τ_e. Therefore, $1/T_2$ in Fig. 2 demonstrates the existence of significant motion of the flux-lines on the time scale of a few tens of μ sec.

The normal state linewidth shown in Fig. 2 is narrow, roughly 7 kHz, suggesting high quality of the crystal. The linewidth in the superconducting state becomes larger than the normal state value, Δf_n. This extra broadening due to the vortices, Δf_v, is extracted from the measured linewidth Δf_m, by using the relation $\Delta f_v=(\Delta f_m^2-\Delta f_n^2)^{1/2}$. The plot of Δf_v is denoted by circles in the inset of Fig. 3. On the other hand, Δf_v for the *stationary* vortices at the regular lattice points can be calculated by taking account of the spatial modulation of the local field in the mixed state. The second moment of the field variation is given as $\sigma_H(T)=\kappa\Phi_0/\lambda(T)^2$, where $\lambda(T)$ is the penetration depth, Φ_0 is a flux quantum, and κ is a numerical factor. The formula for κ has been calculated for $H_{c1}\ll H\ll H_{c2}$ and $0.5\ H_{c1}<H\leqslant H_{c2}$ (Ref. 19). However, for the intermediate magnetic field, for example, $H=1.8$ T in our measurement, κ should be obtained numerically. Using $\lambda(0)=1207$ Å (Ref. 20) and the coherence length $\xi(0)=55$ Å from $H_{c2}(0)=10.5$ T (Ref. 21), we have carried out numerical calculation[18] and obtained $\kappa\approx 0.0228$ for the square lattice at $H=1.8$ T. The linewidth of full width at half maximum is given by $\Delta f(T)=2.36\gamma\sigma_H(T)/(2\pi)$, where γ is the nuclear gyromagnetic ratio of the ^{11}B nucleus, $2\pi\times 13.67$ kHz/Oe.

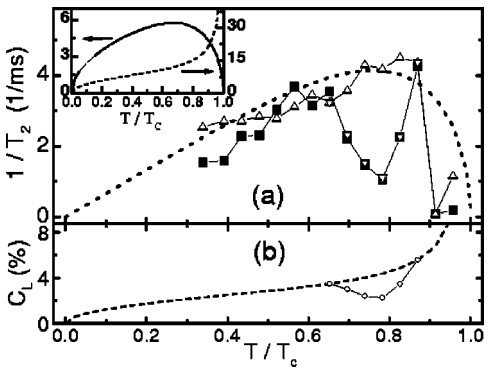

FIG. 4. (a) Analysis of $T_2^{-1}(T)$. Squares, T_2^{-1} after subtraction of normal state contribution from the data in Fig. 2. Dotted line, calculated T_2^{-1} using $T_2^{-1} \approx \gamma^2 \langle h_z^2 \rangle \tau_c$ with $\langle h_z^2 \rangle$ in inset and $\tau_c(T)$ of the dashed line in Fig. 3. Up triangles, T_2^{-1} of the above equation with $\tau_c(T)$ of data (squares) in Fig. 3. Down triangles, generated T_2^{-1} to yield the observed double-peak structure by reducing $\langle u_D^2 \rangle^{1/2}$ for 7.5 K$<T<$10 K. In the inset, solid line, $\gamma \langle h_z^2 \rangle^{1/2}$ in units of kHz, and dashed line, $\langle u_D^2 \rangle^{1/2}$ in units of angstrom (see text). (b) Dashed line, Lindemann number, $c_L \equiv \langle u_D^2 \rangle^{1/2}/d$. Open circles, reduction of $\langle u_D^2 \rangle^{1/2}$ to generate the data of down triangles in (a). Line is a guide to the eye.

Therefore, assuming the two-fluid model for the penetration depth, $\lambda(T) = \lambda(0)[1-(T/T_c)^4]^{-1/2}$, we calculated the expected linewidth, which is shown as a line in the inset of Fig. 3. However, the measured linewidths in the superconducting state are much narrower than the calculated ones for the *stationary* vortices at the regular lattice points. The smaller linewidth in YNi_2B_2C is believed to be due to the vortex motion, as observed for cuprate superconductors.[9,13,14] The reduced linewidth of NMR due to a rapid motion is well known as motional narrowing.[22]

If the vortex motion generates a random fluctuation of the local field, the narrowing effect depends on the characteristic time scale of the vortex motion, τ_c. The linewidth Δf monotonically decreases down to $(\Delta f)^2 \tau_c$ for the rapid fluctuation of vortices, $2\pi \Delta f \tau_c \ll 1$, whereas, it remains unchanged for the slow motion, $2\pi \Delta f \tau_c \gg 1$. For the intermediate time scale of vortex motion, the linewidth is determined as a Fourier transform of the NMR signal decay $S(t)$ (Ref. 22), where $S(t) = \exp[-(2\pi \Delta f \tau_c)^2 \{\exp(-t/\tau_c) - 1 + t/\tau_c\}]$. With Δf given by the field inhomogeneity for the rigid vortex lattice, we vary τ_c until the linewidth of Fourier transform of $S(t)$ is equal to the measured linewidth Δf_v in the inset of Fig. 3. The extracted τ_c is shown in Fig. 3. Note that τ_c is a few microseconds and increases as the vortices become soft toward the vortex liquid. For harmonic oscillation of vortices at a frequency ω, we expect $\tau_c(T) \sim \omega^{-1} \propto c_{66}^{-1/2} \propto \lambda(T) \sim [1-(T/T_c)^4]^{-1/2}$ where c_{66} is the shear modulus of vortex lattice. Thus, τ_c can be fitted to this equation as shown in Fig. 3, the dotted line. We will use it for the analysis of $T_2^{-1}(T)$ in Fig. 4. The magnitude of $\tau_c \sim 10^{-6}$ sec is a few orders of magnitude larger than the typical time scale of flux-line motion, 10^{-9}–10^{-12} sec (Refs. 7 and 11). Since, however, such fast motion would appear to be transparent in the slow precession period of NMR frequency, typically at a few tens of MHz, it is believed that a slow motion may be superimposed upon the fast motion and NMR is only sensitive to the slow motion. This slow motion may originate from pinning.[11]

By subtracting the normal state contribution from the measured value in Fig. 2, $1/T_2$ solely due to the vortex motion is plotted in Fig. 4(a). As discussed earlier, $1/T_2$ is proportional to the fluctuating local field $\langle h_z^2 \rangle$ in the time scale of τ_e. Usually the enhancement of T_2^{-1} is largest when $\tau_e \sim \tau_c$. Not only the value of $1/T_2$ but also the time dependence of echo decay depends on τ_c. For the rapid motion of flux lines, $\gamma^2 \langle h_z^2 \rangle \tau_c^2 \ll 1$, the decay of echo signal is Lorentzian,[22] $M(2\tau_e) \propto \exp(-2\tau_e/T_2)$, with $1/T_2 \approx \gamma^2 \langle h_z^2 \rangle \tau_c$. For the slow motion of flux lines, $\gamma^2 \langle h_z^2 \rangle \tau_c^2 \gg 1$, the decay of echo signal is other than the Lorentzian decay.[11,22] Then, throughout our temperature range we have clearly observed the Lorentzian decay, which suggests that vortices are in the *rapid fluctuation limit*, namely, $\gamma^2 \langle h_z^2 \rangle \tau_c^2 \ll 1$ and $1/T_2 \approx \gamma^2 \langle h_z^2 \rangle \tau_c$ in the mixed state of YNi_2B_2C.

Therefore, in order to understand $T_2^{-1}(T)$ in Fig. 2 we need to account for the temperature dependence of $\langle h_z^2 \rangle$, which is directly related to the vortex displacement in conjunction with $\tau_c(T)$ obtained from the linewidth analysis. If u_i is defined as displacement of the ith flux-line position r_i from a regular lattice point R_i in a plane perpendicular to the c axis, then u_i consists of the *static distortion* u_S and the *dynamic fluctuation* $u_D(t)$ of the flux-line position along the field direction z, namely, $u_i(z) = r_i(z) - R_i = u_S + u_D(t)$. The time scale of fluctuation for u_D is assumed to be τ_c. If the vortex fluctuates by $\langle u_D^2 \rangle^{1/2}$ from its equilibrium position, then the local field fluctuates roughly by $\langle h_z^2 \rangle^{1/2} \approx \Delta H \langle u_D^2 \rangle^{1/2}/(d/2)$ since the spatial field variation $\Delta H = 2.36\sigma_H$, occurs over $d/2$. With the relations of $\Delta H \propto \lambda(T)^{-2}$ and $\langle u_D^2 \rangle^{1/2} \propto \lambda(T)\sqrt{T}$,[23] it is found that $\langle h_z^2 \rangle^{1/2}$ has a broad maximum as shown in the inset of Fig. 4(a). Combining $\langle h_z^2 \rangle$ with τ_c in Fig. 3, we find that $T_2^{-1}(T)$ also has a broad maximum near $T \sim 0.7 T_c$, as shown in Fig. 4(a). In cuprate superconductors, the peak of $T_2^{-1}(T)$ has been reported.[12,14] Although this model explains the general single-peak behavior of $T_2^{-1}(T)$, the temperature dependence of u_D cannot explain the double-peak structure of $T_2^{-1}(T)$ observed for YNi_2B_2C. In cuprate superconductors, not only the single peak[12,14] but also the double peaks[10,11] of $T_2^{-1}(T)$ have been reported, although the latter has not been understood at all.

We notice that the *reduction* of $T_2^{-1}(T)$ from the single-peak behavior occurs in a similar temperature range for the ''peak effect,''[24] which represents a local maximum of the critical current density, $J_c(T)$, near T_c. This indicates that the reduction of $T_2^{-1}(T)$ is presumably due to pinning of vortices resulting in *decrease* of fluctuation part u_D for the pinned vortices. Therefore, reducing $\langle u_D^2 \rangle^{1/2}$ from the $\lambda(T)\sqrt{T}$ dependence for 7.5 K$<T<$10 K, we are able to fit $T_2^{-1}(T)$ to the observed double peak, open down triangles in Fig. 4(a). The reduction of u_D is plotted as the Lindemann number, $c_L \equiv \langle u_D^2 \rangle^{1/2}/d$ in Fig. 4(b). The reduction of $c_L(T)$ due to the pinning is maximally ≈ 0.02. Taking c_L at 10.5 K from Fig. 4(b), we estimate the Lindemann criterion for the vortex liquid to be ≈ 0.067. This agrees with the proposed value $\approx 1/20$ (Ref. 25) for *brittle and fragile* 3D *vortices* as

in YNi_2B_2C. In contrast, this value is much larger for $YBo_2Cu_3O_7$ since vortex lattice is soft and forgiving because of its 2D nature.

Finally, the thermal hysteresis of Knight shift in Fig. 2 has a close relation with the static displacement of vortex position, u_S. The *hysteretic shift* ΔK represents the *remnant distortion* of vortices, Δu_S. Thus Δu_S can be estimated if the field gradient is known. Since ΔK means the shift of the saddle-point field by $\Delta K H_{ext}$, we have $\Delta u_S \approx d\Delta H/(2\Delta K H_{ext})$ and Δu_S is estimated to be a maximum of 10 Å at 5.0 K, which is 3% distortion of vortex spacing d.

In summary, ^{11}B NMR measurements have been performed on a single cystal of YNi_2B_2C for magnetic field parallel to the c-axis. Based on the distinct features of NMR data, we are able to identify the structural change of vortices: vortex liquid just below T_c, through vortex glass, and then to vortex lattice below 4 K. The remarkable vortex dynamics are manifested in the first observation of thermal hysteresis of NMR shift and the double-peak structure of $1/T_2$, as well as the narrow linewidth.

One of the authors (M.L.) wishes to acknowledge financial support of the Korean Research Foundation through 97-001-D00140 and of the Korea Science & Engineering Foundation through 1999-2-114-005-5. This work was partially supported by Center for Strongly Correlated Materials Research at Seoul National University.

*Electronic address: mhlee@kkucc.konkuk.ac.kr

[1] M. Mun *et al.*, Phys. Rev. Lett. **76**, 2790 (1996).
[2] V. G. Kogan *et al.*, Phys. Rev. B **55**, R8693 (1997).
[3] Y. De Wilde *et al.*, Phys. Rev. Lett. **78**, 4273 (1997).
[4] M. Yethiraj *et al.*, Phys. Rev. Lett. **78**, 4849 (1997).
[5] M. R. Eskildsen *et al.*, Phys. Rev. Lett. **79**, 487 (1997).
[6] D. McK. Paul *et al.*, Phys. Rev. Lett. **80**, 1517 (1998).
[7] E. H. Brandt, Rep. Prog. Phys. **58**, 1465 (1995).
[8] C. H. Recchia *et al.*, Phys. Rev. B **52**, 9746 (1995).
[9] A. P. Reyes *et al.*, Phys. Rev. B **55**, R14 737 (1997).
[10] H. N. Bachman *et al.*, Phys. Rev. Lett. **80**, 1726 (1998).
[11] C. H. Recchia *et al.*, Phys. Rev. Lett. **78**, 3543 (1997).
[12] B. J. Suh, D.R. Torgenson, and F. Borsa, Phys. Rev. Lett. **71**, 3011 (1993).
[13] P. Carretta and M. Corti, Phys. Rev. Lett. **68**, 1236 (1992).
[14] E. G. Nikolaev *et al.*, Phys. Rev. B **55**, R8717 (1997).
[15] B. K. Cho *et al.*, Phys. Rev. B **52**, 3684 (1995).
[16] D. E. Maclaughlin, Solid State Phys. **31**, 1 (1976).
[17] B. J. Suh *et al.*, Phys. Rev. B **53**, R6022 (1996); **54**, 15 341 (1996).
[18] K. H. Lee, B. J. Mean, S. W. Seo, K. S. Han, D. H. Kim, Moohee Lee, B. K. Cho, and S. I. Lee (unpublished).
[19] E. H. Brandt, Phys. Rev. Lett. **66**, 3213 (1991).
[20] K. D. D. Rathnayaka *et al.*, Phys. Rev. B **55**, 8506 (1997).
[21] S. V. Shulga *et al.*, Phys. Rev. Lett. **80**, 1730 (1998).
[22] A. Abragam, *The Principles of Nuclear Magnetism* (Clarendon, Oxford, 1961), Chap. 10.
[23] L. I. Glazman and A. E. Koshelev, Phys. Rev. B **43**, 2835 (1991).
[24] A. B. Pippard, Philos. Mag. **19**, 217 (1969); A. I. Larkin and Yu. N. Ovchinnikov, J. Low Temp. Phys. **34**, 409 (1979).
[25] E. H. Brandt, Phys. Rev. Lett. **63**, 1106 (1989).